BMC Genomics

RESEARCH ARTICLE   **Open Access**

Comparative genomic analysis of nine *Sphingobium* strains: insights into their evolution and hexachlorocyclohexane (HCH) degradation pathways

Helianthous Verma[1†], Roshan Kumar[1†], Phoebe Oldach[1], Naseer Sangwan[1], Jitendra P Khurana[2], Jack A Gilbert[3,4] and Rup Lal[1*]

Abstract

Background: *Sphingobium* spp. are efficient degraders of a wide range of chlorinated and aromatic hydrocarbons. In particular, strains which harbour the *lin* pathway genes mediating the degradation of hexachlorocyclohexane (HCH) isomers are of interest due to the widespread persistence of this contaminant. Here, we examined the evolution and diversification of the *lin* pathway under the selective pressure of HCH, by comparing the draft genomes of six newly-sequenced *Sphingobium* spp. (strains LL03, DS20, IP26, HDIPO4, P25 and RL3) isolated from HCH dumpsites, with three existing genomes (*S. indicum* B90A, *S. japonicum* UT26S and *Sphingobium* sp. SYK6).

Results: Efficient HCH degraders phylogenetically clustered in a closely related group comprising of UT26S, B90A, HDIPO4 and IP26, where HDIPO4 and IP26 were classified as subspecies with ANI value >98%. Less than 10% of the total gene content was shared among all nine strains, but among the eight HCH-associated strains, that is all except SYK6, the shared gene content jumped to nearly 25%. Genes associated with nitrogen stress response and two-component systems were found to be enriched. The strains also housed many xenobiotic degradation pathways other than HCH, despite the absence of these xenobiotics from isolation sources. Additionally, these strains, although non-motile, but posses flagellar assembly genes. While strains HDIPO4 and IP26 contained the complete set of *lin* genes, DS20 was entirely devoid of *lin* genes (except *linKLMN*) whereas, LL03, P25 and RL3 were identified as *lin* deficient strains, as they housed incomplete *lin* pathways. Further, in HDIPO4, *linA* was found as a hybrid of two natural variants i.e., *linA1* and *linA2* known for their different enantioselectivity.

Conclusion: The bacteria isolated from HCH dumpsites provide a natural testing ground to study variations in the *lin* system and their effects on degradation efficacy. Further, the diversity in the *lin* gene sequences and copy number, their arrangement with respect to IS6100 and evidence for potential plasmid content elucidate possible evolutionary acquisition mechanisms for this pathway. This study further opens the horizon for selection of bacterial strains for inclusion in an HCH bioremediation consortium and suggests that HDIPO4, IP26 and B90A would be appropriate candidates for inclusion.

Keywords: Hexachlorocyclohexane (HCH), *Sphingobium*, *lin* genes, Xenobiotic compounds

---

* Correspondence: ruplal@gmail.com
†Equal contributors
[1]Room No. 115, Molecular Biology Laboratory, Department of Zoology, University of Delhi, Delhi 110007, India
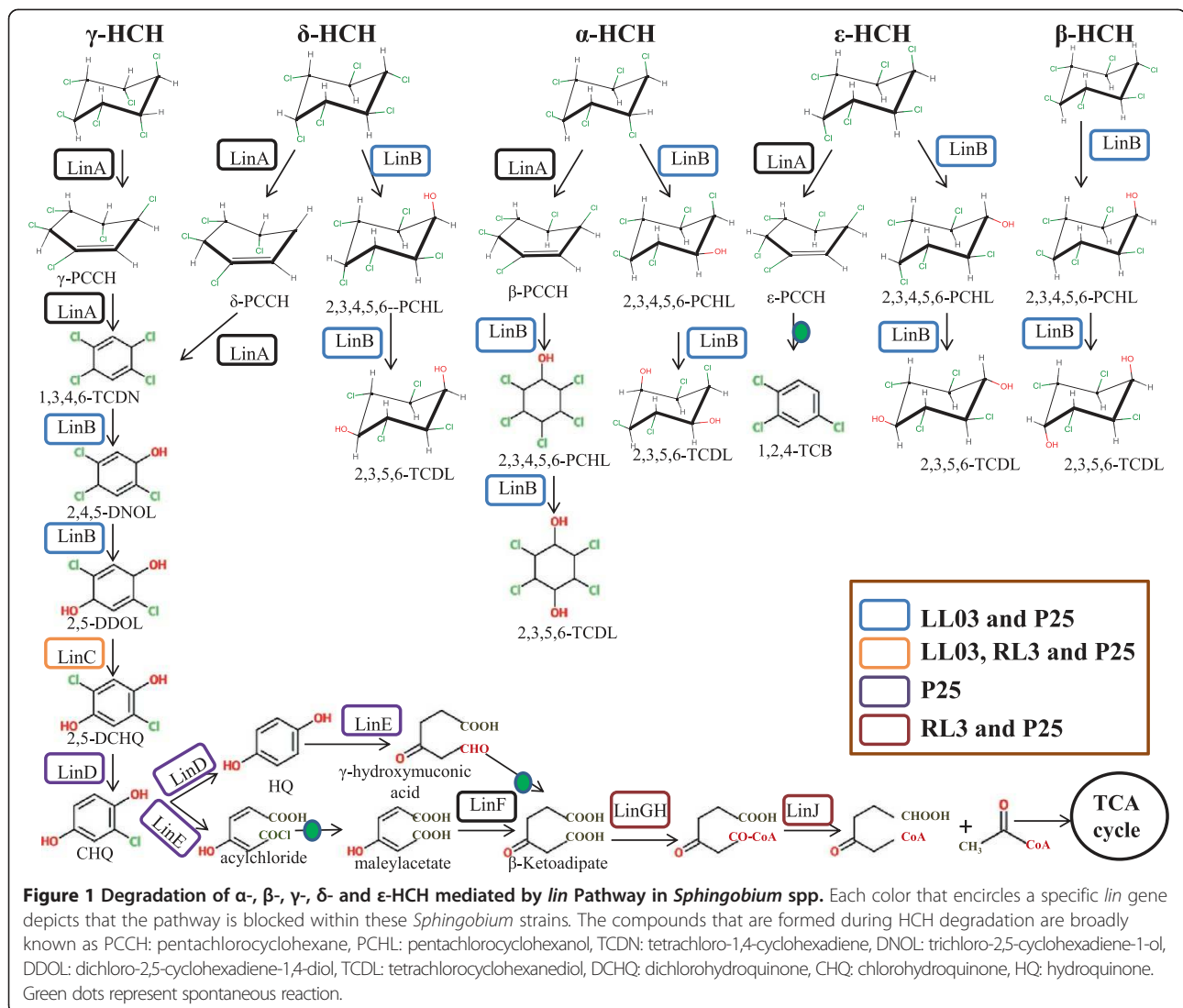Full list of author information is available at the end of the article

Background

The family *Sphingomonadaceae* has been subdivided into five genera: *Sphingomonas*, *Sphingobium*, *Novosphingobium*, *Sphingopyxis* and *Sphingosinicella* [1,2]. To date, the genomes of nearly 40 sphingomonads have been sequenced, which has revealed the genetic basis for the degradation of a broad range of polycyclic aromatic hydrocarbons (PAH) and polysaccharides [3]. However, *Sphingobium* spp. are of particular interest due to their ability to degrade hexachlorocylcohexane (HCH). The majority of HCH isomers (i.e. α, β, δ, ε) are formed during the production of the insecticide lindane (γ-HCH), and have been active pollutants since the 1950s [4]. Among all these isomers, only γ-HCH has insecticidal properties. Purification of γ-HCH (10-12%) from the mixture leads to the formation of HCH muck (88-90% of the total HCH mixture) having mainly α (60-70%), β (5-12%), δ (6-10%), and ε (3-4%) isomers [5]. This has been generally discarded

in the open by the side of industrial units creating a large number of HCH dumpsites between the 1960s to the 1980s around the world [6]. *Sphingobium* spp. are often enriched in HCH dumpsites and have been shown to acquire and maintain genes associated with HCH degradation [7-10].

The degradation potential for HCH isomers has been attributed to the *lin* pathway (Figure 1), which has been studied in detail in both *Sphingobium japonicum* UT26S [11,12] and *Sphingobium indicum* B90A [6]. The *lin* pathway is subdivided into an upper degradation pathway consisting of HCH dehydrochlorinase (LinA), haloalkane dehalogenase (LinB) and dehydrogenase (LinC/LinX), and a lower degradation pathway consisting of reductive dechlorinase (LinD), ring cleavage oxygenase (LinE), maleylacetate reductase (LinF), an acyl-CoA transferase (LinG, H), a thiolase (LinJ) and transcription factors (LinI and LinR). The LinK, LinL, LinM and LinN i.e., a permease,

Figure 1 Degradation of α-, β-, γ-, δ- and ε-HCH mediated by *lin* Pathway in *Sphingobium* spp. Each color that encircles a specific *lin* gene depicts that the pathway is blocked within these *Sphingobium* strains. The compounds that are formed during HCH degradation are broadly known as PCCH: pentachlorocyclohexane, PCHL: pentachlorocyclohexanol, TCDN: tetrachloro-1,4-cyclohexadiene, DNOL: trichloro-2,5-cyclohexadiene-1-ol, DDOL: dichloro-2,5-cyclohexadiene-1,4-diol, TCDL: tetrachlorocyclohexanediol, DCHQ: dichlorohydroquinone, CHQ: chlorohydroquinone, HQ: hydroquinone. Green dots represent spontaneous reaction.

ATPase, periplasmic protein and a lipoprotein respectively, together constitute a putative ABC-type transporter [6].

There is evidence that indicates high levels of polymorphisms in the amino acid sequences of the *linA* and *linB* genes. Further studies have revealed that these differences contribute to the efficacy of HCH degradation and substrate specificity [13]. While there are several strains of sphingomonads isolated from HCH dumpsites with demonstrated differences in HCH degradation ability [8,14], genome-wide comparative analyses to better understand the *lin* pathway, localization of *lin* genes in the genome and methods of recruitment have not yet been undertaken.

In order to understand the evolution of the HCH-degradation pathway, the draft genomes of six *Sphingobium* spp. isolated from HCH dumpsites and the complete genomes of three previously-sequenced, well-studied strains were analysed. Here, we characterize the genetic divergence between these strains in reference to the *lin* catabolic system and auxiliary characteristics associated with bioremediation potential. We also present evidence for possible plasmid and IS*6100* based horizontal gene transfer (HGT) as the method for spread of the *lin* system genes among sphingomonads. Additionally, variation in the *lin* gene sequences is a matter of further investigation for improved degradation ability of these strains.

Results and discussion
Genomic features of *Sphingobium* strains
The genome sizes for the six newly sequenced *Sphingobium* spp. averaged 4.83 Mbp and ranged from 4.08 to 5.89 Mbp, with *S. chinhatense* IP26 maintaining the largest genome (Table 1). These sizes are consistent with existing *Sphingobium* spp. [15]. The variation in genome size can be partially correlated to the presence of genomic islands; IP26 maintained the largest genome and the highest genomic island content, while LL03 had the least (Table 1). This potentially reflects differential degrees of HGT and mobile genetic element acquisition among these strains. UT26S, B90A, IP26 and HDIPO4 all shared high sequence identity (>97%), whereas LL03, P25, RL3 and DS20 have accumulated more sequence variation despite being under similar selection pressures (90-70%) (Figure 2).

CRISPR elements were only found associated with *S. baderi* LL03 (22 spacers) and *S. lactosutens* DS20 (5 spacers). These spacer sequences are known bacterial defense mechanisms against viral and plasmid challenges acquired from foreign invading DNA, with the number of new phage-derived spacers being correlated with phage resistance [16]. However, their spacer sequences had no similarity to known viral phage sequences. Furthermore, LL03 maintained a type II CRISPR element with the *cas9* gene involved in target interference, whereas DS20 had type I CRISPR elements with the *cas3*

gene [17]. Strains LL03 and DS20 were isolated from HCH dumpsites in the Czech Republic and India, respectively, and these strains had two different CRISPR/CAS systems, that may correspond to their different geographical locations. These data also reflected that LL03 should have the greatest phage resistance.

Comparative phylogenetic analysis
Four different phylogenetic methods (16S rRNA gene sequence, single copy gene sequences, tetranucleotide frequency based correlation, and average nucleotide identity (ANI)) were used to analyze the relationships of the nine strains under study (Figure 3). The consensus tree topology obtained by these methods clustered *S. indicum* B90A, *S. japonicum* UT26S, *S. chinhatense* IP26, and *Sphingobium* sp. HDIPO4, with the exception of the single copy gene approach. Notably, these four strains were the only ones with an entirely complete *lin* pathway, thus suggesting convergent evolution through HCH selection pressure. Furthermore, ANI topology supported the grouping of *Sphingobium* sp. HDIPO4 and *S. chinhatense* IP26 as subspecies (≥99.34%) (ANI values within the subspecies >98%) [18]. The other five strains i.e., LL03, DS20, RL3, P25 and SYK6 did not produce a consensus phylogeny, with relationships differing between these approaches; in short, strains with the complete *lin* pathway formed a closed group whereas, the others have diverged. In addition, 16S rRNA and single copy gene approaches may be problematic for differentiation among highly related strains (as these methodologies do not consider the influence of HGT). However, ANI based pairwise comparison has clustered LL03 and RL3 (partial *lin* gene deficient but HCH degraders) in a monophyletic clade with P25 (partial *lin* gene deficient and slow HCH degrader) forming a close relationship. Moreover, DS20 and SYK6 (non-HCH degraders) were clustered together. This suggests that ANI based phylogeny is more appropriate and mirrors their relationship with respect to HCH degradation.
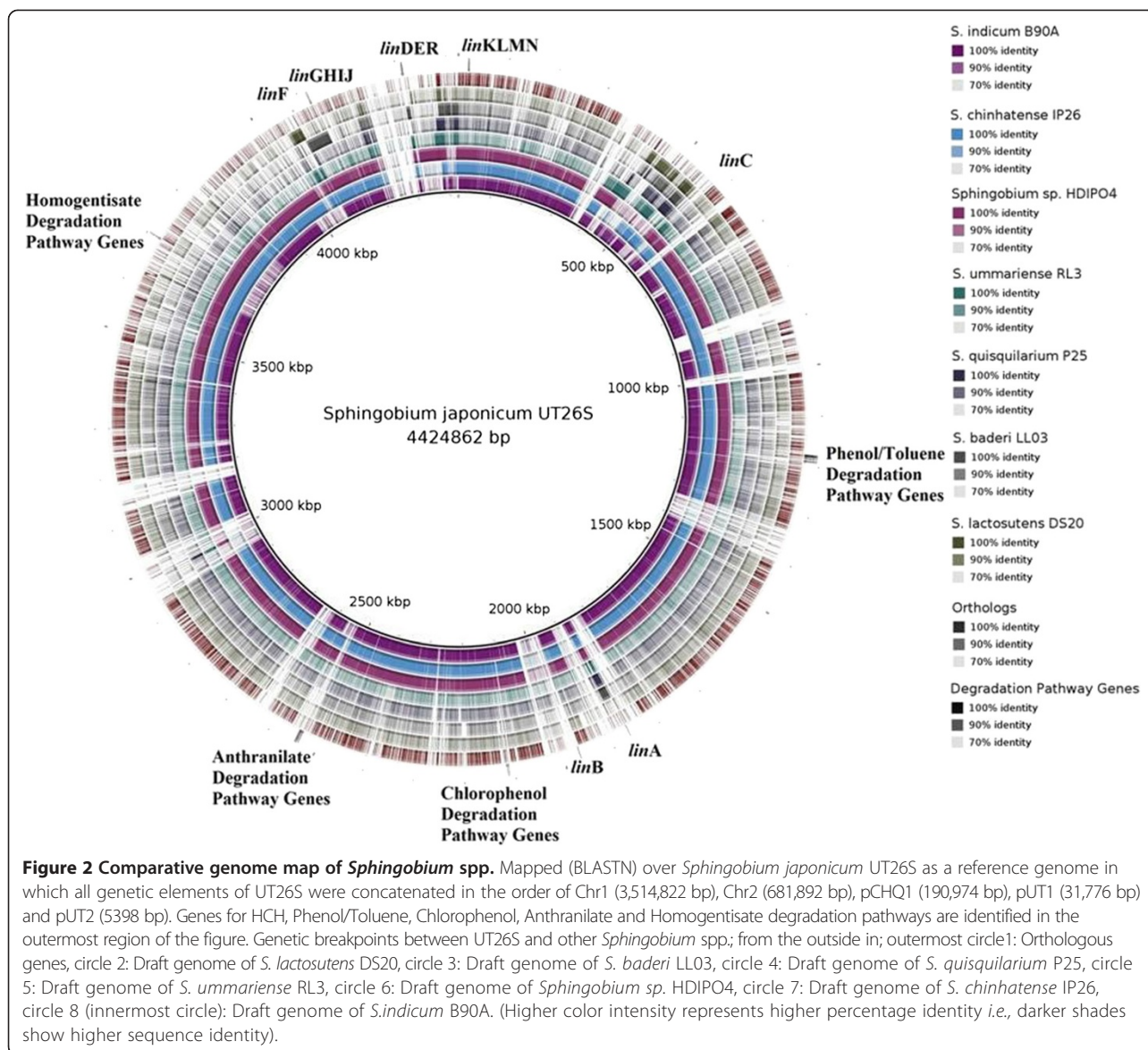
Common gene content and functional profiling of *Sphingobium* spp.
Core genome analysis identified 322 orthologs conserved between the nine genomes. The majority of these genes were involved in housekeeping functions such as the synthesis of ribosomal proteins, DNA replication, transcription & translation machinery, amino acid metabolism and membrane transporters. Core genome analysis for the eight strains that were either isolated from an HCH dumpsite or showed HCH degradation potential (i.e. all except SYK6) predicted 880 orthologs (Figure 2), which suggests a significant increase in genomic conservation (~2.7 times) resulting from the selective pressure of HCH exposure. This conservation is also seen in the degradation potential for other aromatic compounds such as

Table 1 General characteristic features of the *Sphingobium* genomes
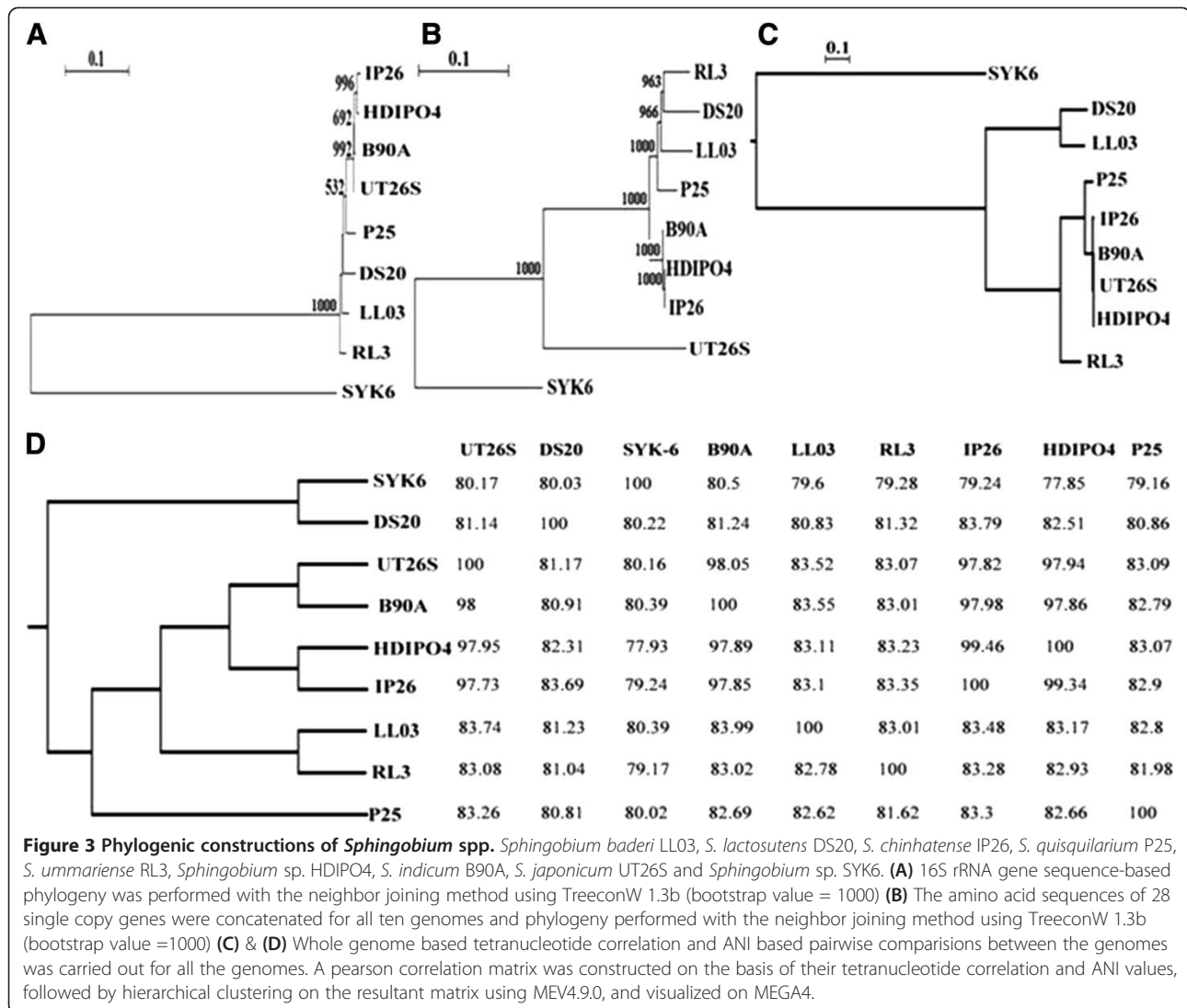
Strains	IP26	HDIPO4	RL3	P25	DS20*	LL03*	B90A	UT26S	SYK6
Project ID	PRJNA208542	PRJNA201012	PRJNA208544	PRJNA201016	PRJNA201649	PRJNA202090	PRJNA50313	PRJDA19949	PRJNA73353
NCBI Accession No.	AUDA00000000	ATDO00000000	AUWY00000000	ATHO00000000	ATDP00000000	ATIB00000000	AJXQ00000000	AP010803 to AP010806	AP012222, AP012223
Source of isolation	HCH Dumpsite, India	HCH Dumpsite, India	HCH Dumpsite, India	HCH Dumpsite, India	HCH Dumpsite, India	HCH Dumpsite, Czech Republic	Rhizosphere Soil, India	Soil Contaminated with γ-HCH, Japan	Waste water of kraft mill pulp, Japan
HCH Degarder	Yes	Yes	Yes	No	No	No	Yes	Yes	No
Genome Size (bp)	5,894,129	4,741,576	4,754,053	4,170,546	5,360,246	4,848,216	4,082,196	4,424,878	4,348,133
G + C content (%)	64.5	65.5	65	64.7	63.6	64	65.8	65.6	66
Predicted CDS	4646 (5161068 bp)	4646 (4105641 bp)	4636 (4152861 bp)	4033 (3644184 bp)	5288 (4682346 bp)	4914 (4312911 bp)	3976 (3570642 bp)	4414 (3929727 bp)	4097 (3825558 bp)
Pseudogenes	10	46	2	70	45	39	-	-	-
Average Gene Size (bp)	903	889	896	903	890	852	886	890	933
% of CDS	87.56%	86.58%	87.35%	87.38%	88.31%	88.96%	87.46%	88.80%	87.98%
IS*6100*	21	18	19	24	15	22	11	5	0
tRNA	66	54	56	49	59	56	54	55	50
rRNA	11	13	12	9	15	12	3	9	6
Genomic islands (bp)	1104688	705420	180116	201158	179141	48062	427792	395714	244403

*Strain having CRISPR element.

Figure 2 Comparative genome map of *Sphingobium* spp. Mapped (BLASTN) over *Sphingobium japonicum* UT26S as a reference genome in which all genetic elements of UT26S were concatenated in the order of Chr1 (3,514,822 bp), Chr2 (681,892 bp), pCHQ1 (190,974 bp), pUT1 (31,776 bp) and pUT2 (5398 bp). Genes for HCH, Phenol/Toluene, Chlorophenol, Anthranilate and Homogentiste degradation pathways are identified in the outermost region of the figure. Genetic breakpoints between UT26S and other *Sphingobium* spp.; from the outside in; outermost circle1: Orthologous genes, circle 2: Draft genome of *S. lactosutens* DS20, circle 3: Draft genome of *S. baderi* LL03, circle 4: Draft genome of *S. quisquilarium* P25, circle 5: Draft genome of *S. ummariense* RL3, circle 6: Draft genome of *Sphingobium sp*. HDIPO4, circle 7: Draft genome of *S. chinhatense* IP26, circle 8 (innermost circle): Draft genome of *S.indicum* B90A. (Higher color intensity represents higher percentage identity *i.e.*, darker shades show higher sequence identity).

benzoate, 1,4-dichlorobenzene, 1,2-methylnapthalene, capro-lactam, toluene and xylene, trinitrotoluene, biphenyl and styrene degradation (Figure 4). Genes involved in the degrad-ation of p-hydroxybenzoate, benzoate, quinate, gentisare, and catechol were also identified in the nine *Sphingobium* genomes (Additional file 1: Table S1). The presence of degradation pathways for phenol/toluene, chlorophenol, anthranilate, and homogentisate are identified in UT26S [19]. These pathways were observed in at least two of the newly sequenced strains (Additional file 1: Table S1). This suggests that these *Sphingobium* spp. possess broad aro-matic compound degradation potential, although we did not observe the presence of these compounds at the HCH dumpsite [20]. The link between these aromatic degrad-ation pathways and the HCH degradation pathway re-quires further investigation.

Functional profiling was used to analyze pathways that were differentially enriched in these strains. For this, a den-dogram was constructed based upon the top 50 subsystems at 0.8% minimum abundance using pearson correlation dis-tance. The analysis revealed that the two-component system for gene expression was highly abundant in all of the *Sphingobium* genomes (Figure 4). This system is known to facilitate adaptation to extreme environmental condi-tions and likely contributes to the ability to survive in con-ditions of high HCH pressure, salinity, and acidity that exist at the HCH dumpsite [9]. Additionally, the nine strains collectively showed an abundance of ABC trans-porters within their genomes. The abundance of these transporters implies that these strains are highly engaged in transport of a wide variety of substrates across extra- and intracellular membranes [21], which is consistent with

Figure 3 Phylogenic constructions of *Sphingobium* spp. *Sphingobium baderi* LL03, *S. lactosutens* DS20, *S. chinhatense* IP26, *S. quisquilarium* P25, *S. ummariense* RL3, *Sphingobium* sp. HDIPO4, *S. indicum* B90A, *S. japonicum* UT26S and *Sphingobium* sp. SYK6. **(A)** 16S rRNA gene sequence-based phylogeny was performed with the neighbor joining method using TreeconW 1.3b (bootstrap value = 1000) **(B)** The amino acid sequences of 28 single copy genes were concatenated for all ten genomes and phylogeny performed with the neighbor joining method using TreeconW 1.3b (bootstrap value =1000) **(C)** & **(D)** Whole genome based tetranucleotide correlation and ANI based pairwise comparisions between the genomes was carried out for all the genomes. A pearson correlation matrix was constructed on the basis of their tetranucleotide correlation and ANI values, followed by hierarchical clustering on the resultant matrix using MEV4.9.0, and visualized on MEGA4.

the *Sphingobium* proficiency for degradation of a wide range of xenobiotics (mentioned above; Figure 4).

Interestingly, HDIPO4 and IP26, which had a close phylogenetic relationship, demonstrated differences in their functional repertoire, based on the top 50 subsystems. This is primarily driven by an increased abundance of 1,4-dichlorobenzene degradation, toluene and xylene degradation, caprolactam degradation, PPAR signaling and atrazine degradation pathways in HDIPO4, which was clustered with functional profiling of P25 and UT26S as they shared these enrichments. Furthermore, lipopolysaccharide biosynthesis, tyrosine metabolism, glycan and glycosaminoglycan degradation pathways were found enriched in IP26 as compared to HDIPO4. This variation suggests that while these strains exhibit similar genomic content, they exhibit differential dominance in their metabolic preferences.

Nitrogen assimilation and the presence of flagellar genes in non-motile *Sphingobium*

The genomes of all the nine strains were found to contain an enrichment of the two component signal transduction system for nitrogen stress response (NtrC pathway) . Additionally, the large subunit of assimilatory nitrate reductase, a key regulator that potentially enables the utilization of nitrate as a nitrogen source, was found to be under diversifying natural selection (dN/dS = 1.09), which suggests that these strains can tolerate low inorganic nitrogen concentrations and are evolving in response to this inorganic nitrogen stress. At high nitrogen concentration, the transmembrane protein *glnC* (*ntrB*/ Histidine kinase) responds to nitrogen availability and phosphorylates *glnG* (*ntrC*), which in turn leads to the activation of *glnA* (glutamine synthetase) [22]. Another key regulator of the pathway is *glnB*, which interacts
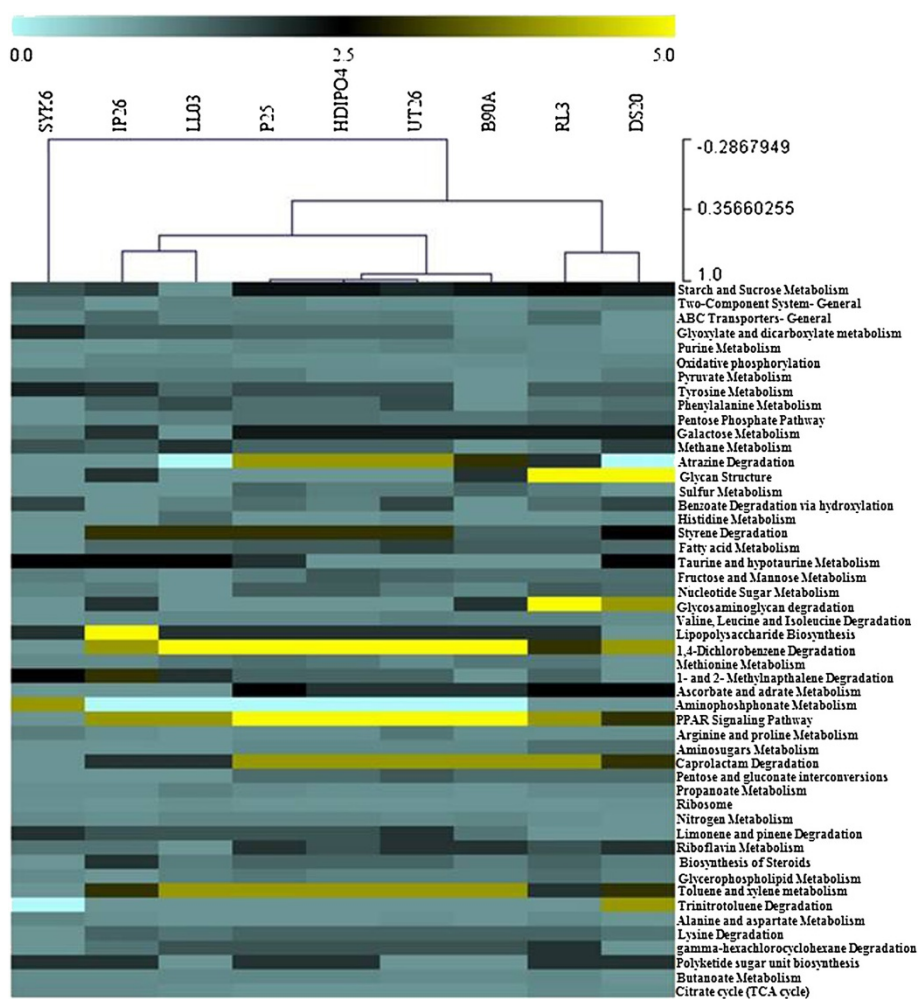
Figure 4 Functional profiling of the *Sphingobium* genomes. Heat map showing the normalized relative abundance of the top 50 subsystems enriched in the nine *Sphingobium* genomes. The strains and enriched pathways were clustered using Pearson correlation with a 0.8% minimum abundance. The color scale represents the relative abundance of gene content for each pathway, normalized by sample mean.

and regulates the activity of *glnC*. When the nitrogen availability is low, *glnB* is subjected to post transcriptional modification by uridylation (mediated by *glnD*). This modification is reversed in N-sufficient conditions [22]. Thus, the presence of *NtrC* pathway and nitrate reductase genes explains the ongoing phenomena of nitrogen assimilation by these strains at HCH dumpsites to acclimatize themselves in such nitrate concentrations. Increasing exposure to elevated hydrocarbon concentrations was found to be positively correlated with the relative abundance of genes associated with nitrogen metabolism [23].

The *NtrC* pathway is also associated with genes regulating chemotactic response, such as *cheY, motA, motB,* and flagellar biosynthesis proteins, such as *flhA, fliO, fliP, fliR* etc. All these genes were also found in the core-genome. *cheY* modulates the cell's ability to interact with the flagellum and controls swimming behavior [24]. Interestingly, while these *Sphingobium* strains are considered non-motile [25-30],

each genome housed more than half of the genes needed for flagellar assembly and functioning. This raises the possibility that they are either in a process of acquiring or losing motility. The abundance of chemotaxis and motility genes has already been demonstrated in the metagenome of the HCH dumpsite [9] from where HDIPO4, IP26, P25, DS20, and RL3 were isolated. However, further analysis is needed to probe the reason for retention or loss of flagellar genes in the *Sphingobium* strains, and to investigate whether *Sphingobium* have the potential to gain motility through acquisition of the remaining genes under the high selective pressure of HCH in the stressed environments.

Recruitment of *lin* pathway through different routes

The genome analysis revealed a mosaic distribution of *lin* genes and IS*6100* elements in HCH-degrading *Sphingobium* spp. coupled with high polymorphism levels in the *lin* genes. This indicates the recruitment of *lin* genes through

different routes in *Sphingobium* spp. under HCH stress, and further that the pathway has not yet stabilized in these strains but is instead subjected to further rearrangements and polymorphisms.

IS*6100*-mediated recruitment based on mosaic distribution pattern of *lin* genes

The IS*6100* elements, known for disseminating *lin* genes through HGT among sphingomonads [7,31-33], were found to be present in all of the newly sequenced strains associated with HCH degradation, including strain DS20 which did not degrade HCH. The number, as determined from the genome sequence, varied from 5 copies in UT26S to 24 copies in P25 (Table 1). The presence of a large number of IS*6100* elements reflects a high degree of genomic rearrangement, as the IS*6100* elements have already been demonstrated to play an important role in the spread and reorganization of the *lin* pathway in sphingomonads [7,10,31-33].

To further explore the mechanism of HGT in the spread and diversification of the *lin* system, we examined the colocalization of *lin* genes with mobile elements such as the insertion sequence IS*6100* and transposons, and their presence on plasmids. In all of strains where *linA* gene was present in, it was found in nearly identical association with IS elements as in UT26S i.e. IS*6100* was found within proximity of <5Kbp. However, in RL3, two IS*6100* copies lies in the same orientation within the above mentioned range. Hence, this suggests that among these strains the association of *linA* with IS*6100* is consistent, but the reason and possible involvement of IS*6100* in the mechanism of duplication of the *linA* gene in RL3 needs to be identified.

In IP26, *linB* was found to be flanked on both sides by IS*6100* (Figure 5A). Additionally, resolvase genes were found at the flanking ends of both of these transposons. Strains LL03 and P25 did not contain the *linB* gene, as confirmed by PCR amplication. Thus, either these strains have yet to acquire the *linB* gene, or, given the flanking IS*6100* elements, it is suggested that the loss of *linB* could have occurred via an intra-chromosomal single homologous recombination between two copies of IS*6100* [19,10].

In HDIPO4, a truncated copy of *linF* along with complete set of *linC* and *linB* was found with an IS*6100* element (length of the segment = 15 Kbp) (Figure 5B). In contrast, in the case of the reference UT26S, these elements were dispersed, with *linF* present on chromosome 2 and *linB* and *linC* on chromosome 1. The association of these three elements suggests that they may have been brought together by IS*6100*-mediated transposition, a hypothesis supported by the fact that HDIPO4 contains a high number of IS*6100* comparable to UT26S (Table 1), and that they may be in the process of forming an operon.

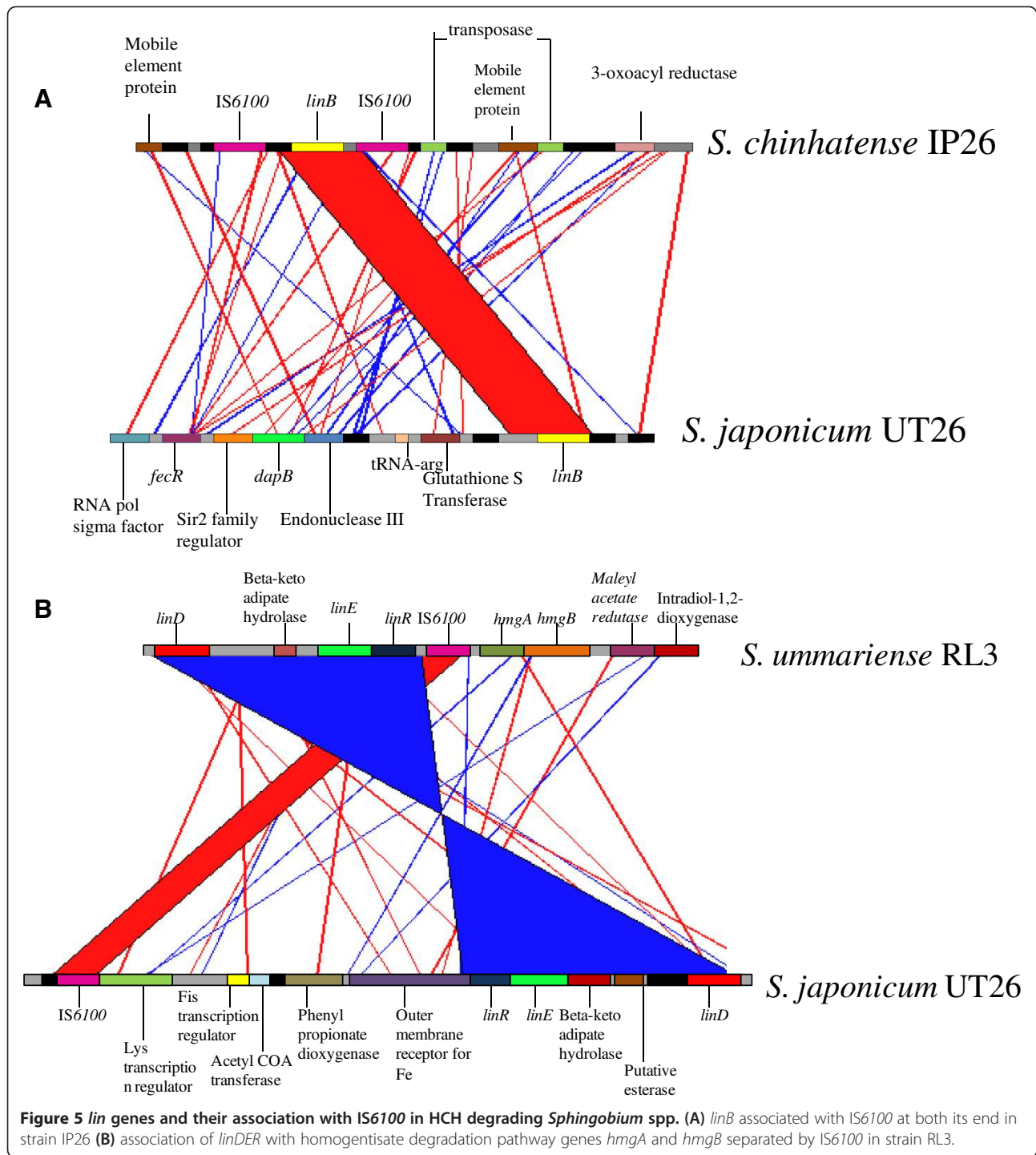Of the three copies of *linDER* present in RL3, one was closely associated with the *hmgB* and *hmgA* genes of the homogentisate degradation pathway, separated by a copy of IS*6100* (Figure 5B). In contrast, in UT26S, *linDER* was housed on a plasmid (pCHQ1), while *hmgB* and *hmgA* were found on chromosome 2 [19]. Therefore, in RL3, it is possible that these two different aromatic compound degradation pathways were brought into close proximity by IS*6100* mediated transposition. Thus, IS*6100*, apart from the spread of *lin* gene system, might be effective in the spread of homogentisate pathways despite the absence of homogentisate selective pressure at the HCH dumpsite, consistent with the fact that already sphingomonads that degrade aromatic hydrocarbons were found to contain catabolic genes associated with IS*6100* [34].

In strain LL03, isolated from the Czech Republic, *linGHIJ* genes were associated with IS*6100*, whereas in the UT26S genome, isolated from Japan, IS*6100* was absent from the region proximal to these lower pathway genes. As IS*6100* is reported to be a key driver in the recruitement of the *lin* system [6], differential organization of the IS*6100* element with respect to *lin* genes for strains from geographically-disparate locations reflects an ongoing IS*6100*–driven evolution of the *lin* system, including the lower degradation pathway components such as *linGHIJ*.

IS*6100* elements have also been found in the genome of DS20, which did not degrade HCH isomers (due to the lack of *lin* genes except *linKLMN*). However, in DS20, the regions flanking the IS*6100* elements comprised a variety of xenobiotic tolerance and degradation genes (i.e., benzene 1,2-dioxygenase, CopA family copper resistance protein, maleylacetatereductase, a putative efflux protein, chlorocatechol 1,2-dioxygenase), which further supports the role of IS*6100* in distributing genes for a broad-range of such functions in *Sphingobium* spp. The fact that DS20, a non-HCH degrader, maintained 15 copies of IS*6100* elements clearly suggests the potential of this strain to acquire *lin* genes through IS*6100* mechanisms in the future.

Plasmid mediated recruitment

In investigating the presence and spread of the *lin* genes, the recently sequenced genome of an HCH-degrader *Sphingomonas* sp. MM-1 is of interest as it was found to have five plasmids housing the genes of the *lin* pathway [35]. In the MM-1 genome, the *linF* was found on pISP0; *linA, linC,* and a truncated *linF* on pISP1, *linDER* on pISP3, and *linB, linC,* and another truncated *linF* on pISP4 [35] and *linGHIJ* was found on pISP0. Genes for an ABC transporter were found on the chromosome, but these did not share at least 80% identity to the *linKLMN* genes of UT26S. In addition to this, in strain UT26S, HCH-specific genes of the *lin* pathway were found to be housed on regions unique to the UT26S genome [19]; with *linA, linB, linC* genes in chromosome 1, *linF* on chromosome 2, and *linDER* on the plasmid pCHQ1 [19]. The lower pathway genes, including *linGHIJ* and *linKLMN* were found on

Figure 5 *lin* genes and their association with IS*6100* in HCH degrading *Sphingobium* spp. (A) *linB* associated with IS*6100* at both its end in strain IP26 **(B)** association of *linDER* with homogentisate degradation pathway genes *hmgA* and *hmgB* separated by IS*6100* in strain RL3.

chromosomes 2 and 1, respectively, in regions that were conserved among sphingomonads [19].

Genome recruitment plots were created to map the raw reads of the six novel-sequenced strains to *Sphingobium* plasmid sequences to investigate the possibility of these plasmids playing a role in transfer of the *lin* genes. MM-1 plasmids pISP3 and pISP4 in particular were found to have a high percentage of coverage which was maximum

with *S. ummariense* RL3 (Figure 6). As pISP3 houses *linDER*, it is highly probable that plasmid uptake and duplication may explain the triplication of *linDER* in RL3. The recent metagenomics analysis of the HCH dumpsite also reflected the enrichment of pISP3, suggesting its availability for other sphingomonads strains present at the HCH dumpsite [10]. Furthermore, pISP4 encodes *linB, linC,* and *linF,* and similarly shows a high
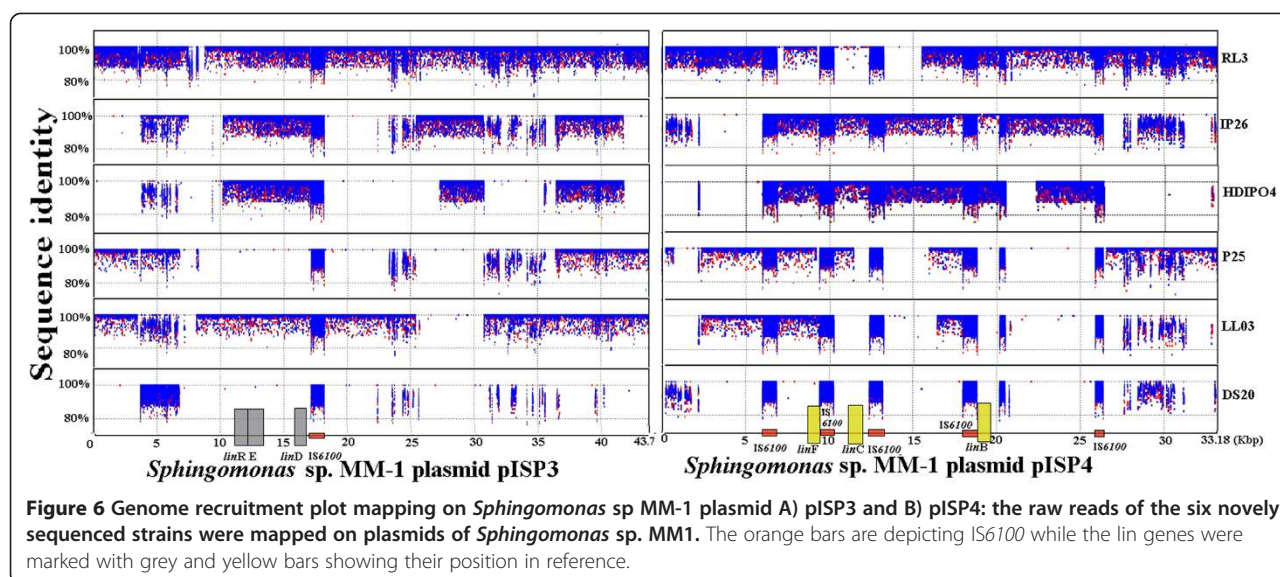
Figure 6 Genome recruitment plot mapping on *Sphingomonas* sp MM-1 plasmid A) pISP3 and B) pISP4: the raw reads of the six novely sequenced strains were mapped on plasmids of *Sphingomonas* sp. MM1. The orange bars are depicting IS*6100* while the *lin* genes were marked with grey and yellow bars showing their position in reference.

degree of coverage by RL3. Consistent with the absence of *linC* from the RL3 draft genome, which was confirmed by PCR amplification by using the primer 5′-GCGG ATCCGCATGTCTGATTTGAGCGGC-3′ and 3′-GCCT CGAGTCAGATCGCGGTAAAGCCGCCGTC-5′, there is a gap in the coverage seen in the plasmid region containing *linC* (11,370 to 12,122 bp), which is a region flanked by two IS*6100* elements in MM-1 (Figure 6). This points to the possibility that the plasmid has undergone either acquisition in MM-1 or looping out from RL3 of the *linC* gene during the course of evolution, mediated directly by IS*6100*. Mapping the raw reads of the six newly-sequenced *Sphingobium* strains to the plasmid sequences for MM-1 and UT26S, several of the MM-1 plasmids, but none of the UT26S plasmids demonstrated a high degree of coverage. Additionally, the proportionally higher presence of *lin* genes on plasmids in MM-1 than in UT26S suggests that strain MM-1 acts as a reservoir for plasmids allowing for the effective spread of the *lin* system, and thus may be an important strain to include in the consortium development as a potential disseminator of the *lin* system. Also, strains sharing similar arrangement profile of *lin* genes with MM-1 i.e., RL3, IP26 and HDIPO4, should be included into designing a consortium.

Strains in transition to acquire *lin* pathway

Of the nine sphingomonads under study, seven possessed components of the upper HCH degradation pathway to varying degrees of completion, and two, SYK6 and DS20, were completely devoid of them (Additional file 1: Table S2). SYK6 did not contain any components of the *lin* system and the DS20 genome contained only genes of the lower *lin* pathway- *linKLMN* an ABC transporter. Of the HCH-degraders, not every strain was found to house the complete array of *lin* genes characterized in UT26S or

B90A. For instance, the P25 genome lacked *linB, linC, linDER, linGH, linI* and *linJ* genes while, strains RL3 and LL03 both lacked *linC* and LL03 lacked *linB,* as confirmed by PCR amplificiation (Additional file 1: Table S2). The differential composition of the *lin* system between these strains may be indicative of different steps in the evolution of the *lin* pathway, with IP26 in the stage of probable homologous recombination and looping out of *linB,* while LL03 shows potential gain of *linGHIJ* through IS*6100*-mediated HGT. Strain DS20 possesses ABC transporters and shows potential for acquisition of the *lin* genes, as it holds 15 copies of IS*6100,* while P25, in addition to the ABC transporter, has *linA* and *linF* but is yet to acquire the other *lin* genes.

lin system sequence diversity and its effect on metabolic efficiency

Upper *lin* pathway

The upper pathway genes *linA, linB* and *linC* degrade γ-HCH and α-HCH, and additionally *linB* acts on β-HCH, leading to the formation of β-2,3,4,5,6-pentachlorocyclohexanol (β-PCHL) (Figure 1). As α- and β-HCH form the major components of contamination at the HCH dumpsite (>80%), both *linA* and *linB* are extremely important enzymes encoding HCH dehydrochlorinase and haloalkane dehalogenase, respectively (Figure 1). To gain deeper insights into the *lin* gene sequence diversity and its impact on HCH degradation, the genetic divergence of the *lin* system components was analyzed with respect to the copy number and nucleotide sequence divergence of the *lin* genes in both upper and lower degradation pathways, using B90A as a reference.
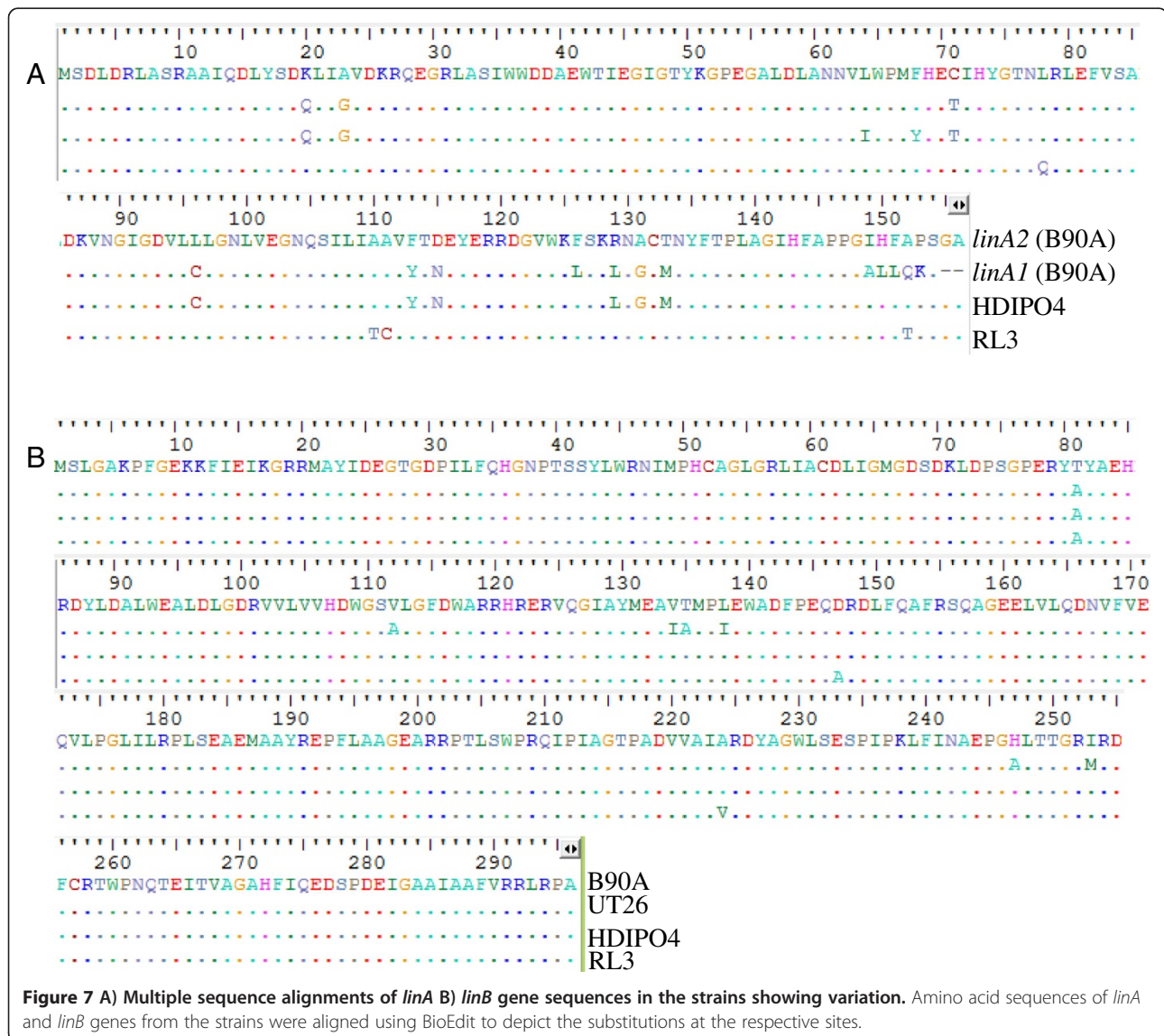
The highest level of divergence in the upper HCH degradation pathway *lin* genes was reported for the *linA* gene encoding for HCH dehydrochlorinase in B90A [36]. The two previously characterized *linA* variants observed in

B90A differed by 10% of their amino acid sequence, and were named *linA1* and *linA2.* The functional aspects of these variants have been well characterized, as they show enantioselectivity in (±) α-HCH degradation, with LinA1 selective for the (+) and LinA2 for the (-) α HCH [37]. Also, the degradation ability of LinA1 was found to be lower than that of LinA2 [36]. Among all the *lin* genes of the upper pathway, *linA* in the present study was found to be most diverged in HDIPO4, in which it appeared to be a hybrid of the two variants (*linA1* and *linA2*) with 94.8% sequence similarity to *linA1* and 92.9 to *linA2*. Near to the catalytic dyad D25 and H73 critical for its enzymatic activity, the HDIPO4 *linA* was found to be identical with *linA1* [38]. However, the C-terminal region corresponded to *linA2* (Figure 7A). This hybrid copy, now marked as *linA3*, requires further experimentation, but might be responsible for the comparatively better dehydrochlorination

activity of HDIPO4 against α- and γ-HCH, as reported earlier [14].

Apart from this divergence of the *linA* sequence in HDIPO4, not such changes to the *linA* gene sequences were observed; all strains showed 100% sequence similarity to that of the *linA2* gene [36] with the exception that *linA2* of RL3 showed a single substitution of L78Q. It is important to mention here that the *linA* gene has already been reported to be under continuous selection pressure and a large number of variants of this gene exist [7,32,13,39] and better variants of *linA* may be used for developing enzymatic bioremediation system for HCH.

In contrast to *linA*, there were less variations in *linB* sequences among strains under study. The sequence differences among *linA* and *linB* genes among different *Sphingobium* spp. are particularly interesting in light of

Figure 7 A) Multiple sequence alignments of *linA* B) *linB* gene sequences in the strains showing variation. Amino acid sequences of *linA* and *linB* genes from the strains were aligned using BioEdit to depict the substitutions at the respective sites.

findings that marginal differences in the amino acid sequences of *linB* in UT26S [40], SP⁺ [41], B90A [31], BHC-A [42] and M1205 [43] can alter the efficacy and substrate range, with the former group degrading β-HCH to β-PCHL and the latter group taking the pathway beyond PCHL to TCHL. HDIPO4 housed two identical *linB* copies with a T81A substitution and overall 99.6% similarity to B90A while RL3 *linB* gene had 98.9% identity, with three substitutions (T81A, D147A and A224V) as compared to *linB* of B90A (Figure 7B). Here, the copy number difference is suspected to have a more impact, as the two copies of *linB* might explain the high β-HCH degradation efficacy of HDIPO4 [14,27]. Apart from these two strains, no such diversity was observed, thus demonstrating the stability of *linB* gene in the population. *linC*, which encodes for HCH dehydrogenase was most conserved among the genes of the upper degradation pathway and demonstrated only a single substitution: Y172C in case of IP26. In any case these studies reflect that *linA* genes are more prone to evolutionary changes under HCH stress and have not stablized yet.

Lower *lin* pathway

The lower pathway of γ-HCH degradation begins from 2,5-Dichlorohydroquinone (2,5-DCHQ) an intermediate of γ-HCH (Figure 1), which is mineralized by the lower pathway *lin* genes (*linDER, linF, linGHIJ,* and *linKLMN*) [6]. In contrast to the upper degradation pathway, very less is known about the divergence and polymorphisms of the genes of the lower degradation pathway.

Among all the *lin* genes of the lower pathway, *linF* was the most highly conserved, as its amino acid sequence was 100% identical in all genomes (Figure 8). In the *linDER* operon, the set of *linD* genes similarly showed minimal divergence, with the IP26, RL3, and LL03 genes sharing a substitution of N82S, and additionally IP26 having a substitution Q30P. Further, *linR* and *linE* had very little divergence; *linR* diverged only in one substitution in HDIPO4 (L12P) and *linE* was 100% identical in all strains. This highlights the fact that the *linDER* operon, which makes up the backbone of the downstream HCH degradation pathway, remained highly stable during the course of evolution. A greater degree of the variation of this operon was found, however, in copy number, as RL3 and HDIPO4 housed three and two copies, respectively (Figure 8 & Additional file 1: Table S2).

In particular *linGH, linI* and *linJ*, which mediate the later stages of the lower degradation pathway, i.e., conversion of β-ketoadipate to succinyl CoA and acetyl CoA (Figure 1), showed variation in the sequences of *linH* and *linI*, whereas *linG* and *linJ* sequences were 100% conserved among all these strains. Here, *linH* of HDIPO4 and IP26 were similar to each other, and both diverged from B90A with 99.06% identity. They held two substitutions (I31V and N171H) while LL03 shared the I31V substitution and additionally had a N131D substitution. *linI* was found to be identical in HDIPO4 and IP26, with a single substitution (A188T) and 99.62% identity to B90A, while LL03 had two substitutions (A9T and A185V) and 99.25% identity. However, the significance of sequence divergence in *linG, linH, linI,* and *linJ* genes among these strains is yet to be investigated.

Another important *lin* gene system of the lower pathway is the ABC transporter system i.e., *linK, linL, linM,*
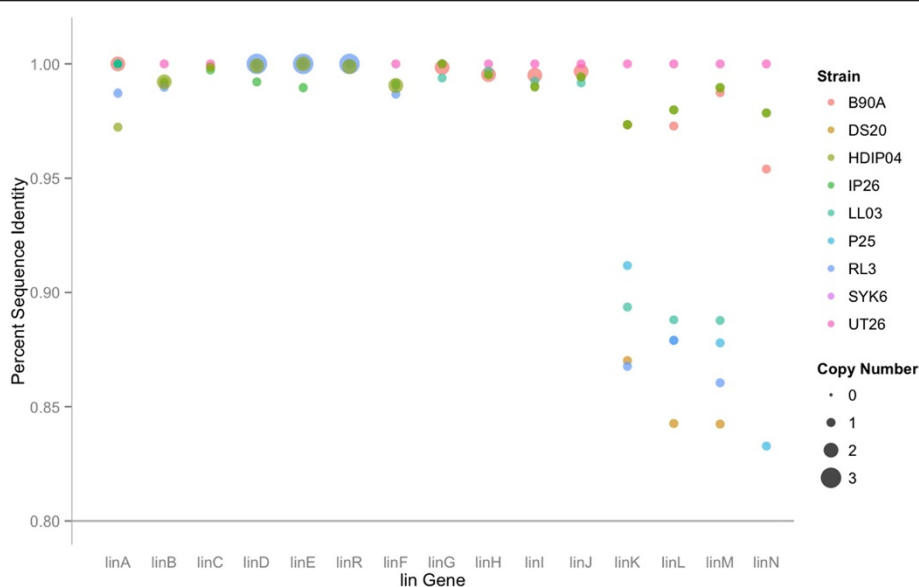

Figure 8 Genetic sequence and copy number variation of *lin* genes: The genetic divergence, as quantified by percentage nucleotide identity to the archetypal strain UT26, and copy number variation in *lin* genes across the nine *Sphingobium* strains under study.

and *linN,* which encode a permease, ATPase, periplasmic protein, and lipoprotein, respectively. This ABC transpoter system is very important as it allows for the transport of HCH isomers and clearance of dead-end metabolites of HCH from the cell [21]. Out of the entire *lin* system these genes have shown the highest level of of divergence with *linK* at 86.8% in RL3, *linL* at 84.3% in DS20, *linM* at 84.2% in DS20 and *linN* at 83.3% in P25. Based on the prevalence of similar but non *lin*-specific ABC type transporters which are found by sequence identity searches across a variety of microbial species, it is hypothesized that the *linKLMN* operon derived from convergent evolution in response to environment changes. With the introduction of the HCH to the environment, pre-existing ABC-type transporters were likely recruited to the HCH degradation pathway, and thus several genetic variants might have undergone convergent evolution to select for transporters with increased efficiency for HCH-metabolite efflux, and these later generation genes were the one that subsequently underwent HGT. This is in contrast to the likely origin of the *linDER* operon, which encodes more highly HCH-specific enzymatic functions and is almost perfectly conserved, and thus was likely generated once, and spread through HGT from a single genetic ancestor. The *lin* pathway shows a characteristic pattern in which the upper HCH degradation pathway was diverged along a gradient from the most, *linA* (highly diverged) to the least, *linC* (least diverged). While in the lower degradation pathway *linKLMN* was the most highly diverged, followed by *linGHIJ, linDER* and *linF* respectively.

In literature, the degradation ability of these strains under consideration is in the order: HDIPO4>IP26>RL3. In order to further substantiate the relationship between *lin* system diversity and degradation efficiency, principle component analysis (PCA) was performed on the copy number and sequence divergence for these strains, with HCH degradation plotted as a supplementary variable to visualize correlation. The analysis demonstrated a close grouping of the four *lin*-deficient strains, i.e. SYK6, DS20, LL03, and P25 under PCA 1 and 2 (accounting for 32.57 and 24.99% of the variation in these strains, respectively) (Figure 9A). HDIPO4 and IP26 were colocalized in quadrant 4, opposite from the non-degrader cluster in terms of both dimension 1 and dimension 2, which is appropriate given that these two strains have degradation rates documented to be faster than archetypal strains UT26S and B90A [14] (Figure 9A). While copy number variation for *linF, linDER,* and *linB* were mapped most closely to the HCH degradation vector (Figure 9B), the copy numbers for *linC, linGHIJ* and again *linB* played a more important role in differentiating these strains, as they correlated significantly to PCA1 (p values 5.897964e-05, 2.998361e-02, and 1.206315e-02,

respectively). In terms of sequence, *linA* and *linR* showed high correlation to degradation ability (Figure 9B), while *linL, linM, and linK* were significantly correlated to PCA1 (p values 1.340825e-04, 2.934465e-04, 4.192410e-04, respectively) and *linI, linH, linC, linB,* and *linF* were the most significant contributors to PCA2 (p values 0.0007954298, 0.0010696278, 0.0105835905, 0.0107931486, 0.0222238515, respeictvely). This suggests that while variation can be seen throughout the *lin* pathway and the copy number of *linF, linDER* and *linB* sequence for *linA* and *R* might have the most impact in optimizing the efficacy of an HCH enzymatic bioremediation system.

Genes under diversifying natural selection

To identify the substitutions that have fixed along the independent lineages and their direction of evolution, dN/dS (rate of non-synonymous over synonymous substitution) analysis was performed for sets of orthologous genes, and in particular those responsible for the degradation of HCH, phenol/toluene, homogentisate, chlorophenol and transposons/integrases (Figure 10). The genes of interest found to be under diversifying selection (dN/dS > 1) includes those for Fe(II) dependent oxygenase, ABC transporters, assimilatory nitrate reductase, and general secretory pathway protein. These genes are largely associated with stress tolerance. As mentioned earlier, ABC transporters are involved in uptake of high molecular weight pharmacological agents including xenobiotic compounds [44]. Hence, these transporters and their activity are crucial for their capability of HCH degradation and other aromatic compounds and likewise, their positive selection indicates the importance of their function in the HCH-stressed environments from which these bacterial strains were isolated. Additionally, nitrate reductase catalyzes the conversion of nitrate into free nitrogen and likely would enable the *Sphingobium* spp. to more effectively enact a nitrogen stress response. Finally, the diversification of genes such as oxygenases, secretory pathway proteins and translocase components adds to the sphingomonads skill of degradation of a wide range of aromatic compounds. Notably, only *linH* has shown the dN/dS > 1, while the other *lin* genes did not. This clearly indicates that under strong HCH pressure, the whole *lin* pathway is likely to get stabilized in the population with more synomous substitutions compared to non-synonomous ones and tends to be retained in the population.

Conclusions

In sequencing the genomes of six novel *Sphingobium* species and comparing these to the known genomes of three other *Sphingobium* species, this study has begun to probe the natural variation in the *lin* pathway for HCH degradation. Analysis of the variation in the *lin* system, as well as in the phylogenetic relationships, core genomes,
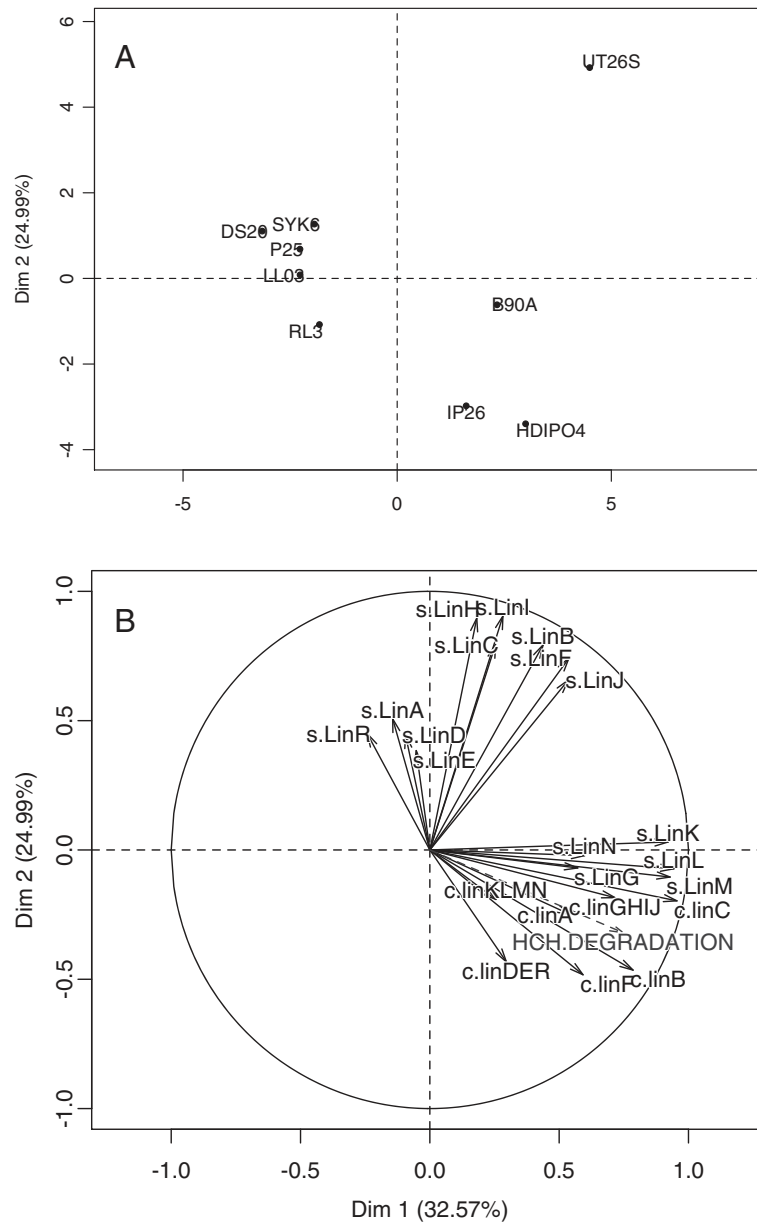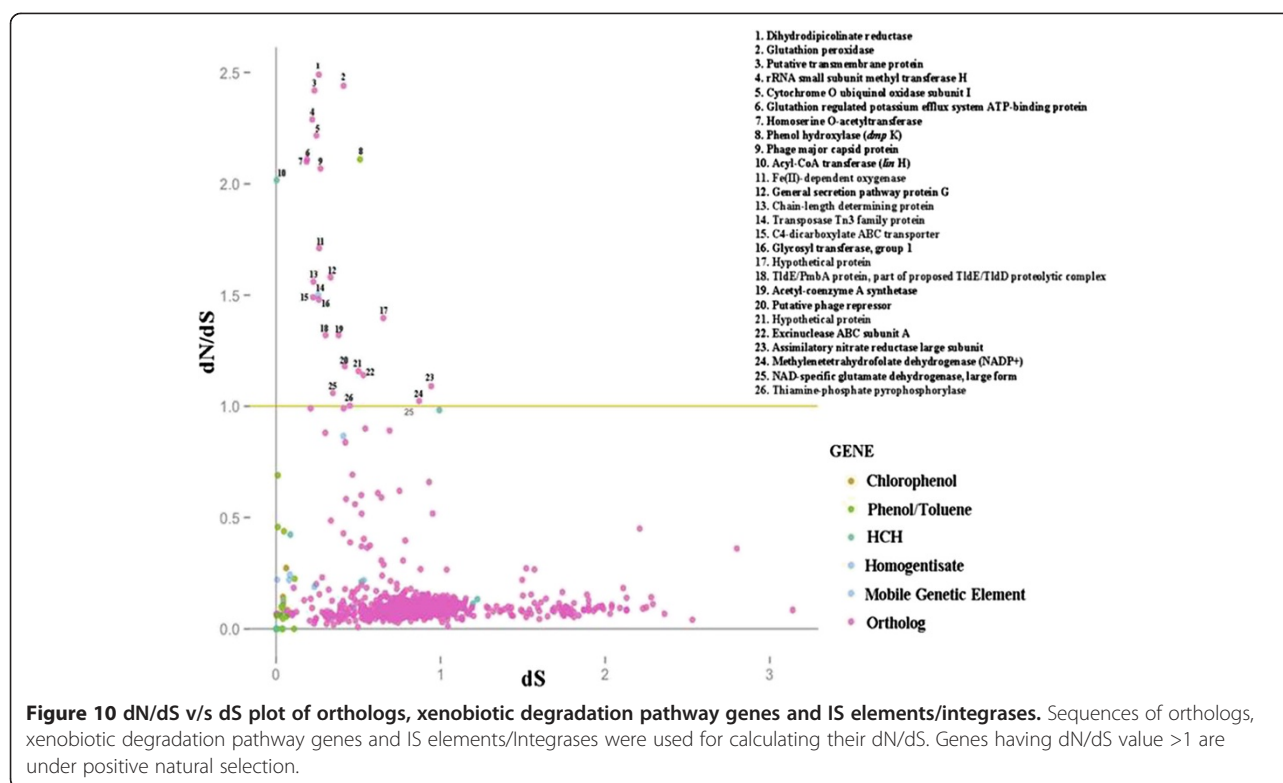
Figure 9 Principal Component Analysis of genes involved in HCH degradation pathway. (A) PCA individual factor plot showing the grouping of the nine *Sphingobium* strains based upon the sequence divergence and copy number of the set of *lin* genes. Principle components 1 (accounting for 30.87% of the variation of the strains) and 2 (14.47%) were chosen as the separation of the strains by these PCs demonstrated the highest fidelity to known HCH degradation ability. **(B)** PCA variable factor plot using principle component 1 and 2, showing the contribution of the lin genetic sequences (s.linA, s.linB…) and copy number (c.linA, c.linB…) to the variation of the nine *Sphingobium* strains. HCH degradation ability was plotted as a supplementary categorical variable (not factored into the PCs), with non-HCH degraders coded as 0, partial degraders as 1, and complete degraders as 2.

and functional profiles of these bacterial strains demonstrated unique characteristics of B90A, HDIPO4 and IP26 which could explain their higher efficacy as the degraders of HCH isomers. The information thus obtained can now be used to select these better-performing strains for the development of a bacterial consortium for on-site bioremediation of the HCH dumpsites. Focusing on the *lin* system, analysis of the similarities in the *lin* genes sequences

and varying copy numbers between these strains has identified variations in the specific genes as key differentiators and these key components will be of critical interest as the most effective targets for optimization of an enzymatic bioremediation system. The analysis so far made reflect that better *linA* and *linB* variants can eventually be the ideal candidates for developing an enzymatic bioremediation system. Moreover, this study has uncovered evidence for genus-level

Figure 10 dN/dS v/s dS plot of orthologs, xenobiotic degradation pathway genes and IS elements/integrases. Sequences of orthologs, xenobiotic degradation pathway genes and IS elements/Integrases were used for calculating their dN/dS. Genes having dN/dS value >1 are under positive natural selection.

HGT of plasmids housing components of the *lin* system, specifically between *Sphingomonas* sp. MM-1 and RL3. The additional *lin*-deficient strains are of further importance as they demonstrate varying degrees of acquisition of the *lin* system and will be useful in future homologous recombination studies to work with manipulated pathway completion through introduction of synthetic *lin* genes.

Methods

Selection and sequencing of the *Sphingobium* genomes

Six *Sphingobium* strains isolated from HCH dumpsites and demonstrating a range of HCH degradation abilities were selected for genome sequencing. Five of these *Sphingobium* strains i.e. *S. lactosutens* DS20[T] [26], *S. chinhatense* IP26[T] [27], *S. ummariense* RL3[T] [28], *S. quisquilarium* P25[T] [29], and *Sphingobium* sp. HDIPO4 were isolated from an HCH dumpsite in Chinhat village, Lucknow, India whereas, *Sphingobium baderi* LL03[T] [30], was isolated from an HCH dumpsite in Spolana, Czech Republic. In addition to these six strains, the genomes of an additional three strains: *Sphingobium indicum* B90A [45], *Sphingobium japonicum* UT26S [46], and *Sphingobium sp* SYK6 [47], were included as references in the study.

Genomic DNA was extracted from 5 ml pure culture pellets grown in Luria Bertani at 28°C until O.D. 1.0 or 1.2 using the SuperCos method [48]. DNA concentrations were quantified using NanoDrop spectrophotometer (NanoDrop

Technologies Inc, Wilmington, DE, USA). For all the genomes, sequencing was performed using both the Illumina HighSeq 2000 and 454 GS-FLX Titanium platforms. For sequencing, a 2 Kbp paired end sequencing library was constructed, yielding ~100× coverage for each genome. An additional three *Sphingobium* genomes i.e. *Sphingobium japonicum* UT26S, *S. indicum* B90A and *Sphingobium* sp. SYK6 were retrieved to be used as references for this comparative analysis (Table 1).

Genome assembly, annotation, and functional profiling

The sequencing data were assembled using ABySS 1.3.3 [49] at various k-mer lengths optimized for each genome. Detailed statistics of the genome assemblies are provided in Table 2. The assembly was validated using paired-end information on the Burrows-Wheeler Aligner 0.5.9 (BWA) [50]. The accession numbers and details of the genomes used in this study are provided under Table 1 [51-56]. CDS were predicted using Glimmer-3 [57] and annotated on RAST 4.0 Server [58] for both the draft and complete genomes.

For functional profiling, coding sequences were extracted from the RAST server for all the genomes, and orthologous genes were determined using all-versus-all BLASTP at default parameters [59]. This was validated by using CD-HIT [60] to produce sets of non-redundant representative sequences (query coverage ≥80%, 0.8 sequence

Table 2 Detail statistics of genome assembly of *Sphingobium* spp.

Organism (Genome status)	Assembler	K-mer length	No. of Contigs/Chromosomes & Plasmids	N50 (in Kb)
S. baderi LL03 [T] (Draft)	ABySS 1.3.3	47	92	269
S. lactosutens DS20 [T] (Draft)	ABySS 1.3.3	53	110	303
Sphingobium sp. HDIPO4 (Draft)	ABySS 1.3.3	53	143	172
S. chinhatense IP26 [T] (Draft)	ABySS 1.3.3	61	236	142
S. quisquilarium P25[T] (Draft)	ABySS 1.3.3	47	181	45
S. ummariense RL3[T] (Draft)	ABySS 1.3.3	57	139	363
S. indicum B90A[T] (Draft)	ABySS 1.2.7	41	149	54.5
S. japonicum UT26S[T] (Draft)	PHRAP and CONSED	-	Chromosome 1 (3,514,822 bp), chromosome 2 (681,892 bp), pCHQ1 (190,974 bp), pUT1 (31,776 bp) ans pUT2 (5,398 bp)	-
Sphingobium sp. SYK6	PHRED/PHRAP/CONSED	-	chromosome 1 (4,199,332 bp) and pSLGP (148,801 bp)	-

identity cut-off). The putative protein coded for each cluster was identified through performing BLASTP on a representative amino acid sequence from each cluster. Comparison of the annotated genomes were also carried out in MicroScope server [61].

Further, the coding sequences were processed for functional annotation using the bi-directional best-hit (BBH) assignment method on KEGG Automatic Annotation Server (KAAS) [62]. This annotation was then used for biological family construction using protein family prediction on MinPath [63]. The top 50 subsystems were selected based on normalized values obtained by dividing with the lowest value for the genes in the respective pathways. Finally, the nine *Sphingobium* strains and enriched pathways were clustered heirarchially using Pearson correlation with 0.8% minimum abundance and a heat map was constructed in MeV4.9.0 [64]. Genomic Islands (GIs) were analysed using the IslandViewer software tool (http://www.pathogenomics.sfu.ca/islandviewer) [65]. The CRISPR Finder online server was used to identify CRISPR elements in the draft genomes [66], which were further analyzed to trace their sources.

Phylogenetic analysis of *Sphingobium* spp.
The phylogenetic analyses were performed using four different methods.

i) **16S rRNA gene sequences:** which were retrieved using BLASTN (E-value = 10^{-5}) [59]. The 16S rRNA sequences were aligned using CLUSTALX [67] and subsequently a phylogenetic tree was constructed using the TreeconW software package version 1.3b [68] with the Jukes & Cantor model (1969) [69] and Neighbor Joining algorithm (bootstrap value = 1000).

ii) **Single Copy Gene Sequences:** The amino acid sequences of 28 universally present single copy genes (*dnaA, frr, gyrB, infB, mnmA, nusA, pheS, rplB, rplC, rplM, rplS, rpoA, rpsB, rpsC, rpsH, rpsI, rpsJ, rpsS, trmD, tef, ychF, alaS, rplE, uvrC, lepA,*

rplI, rplP and *rplD*) were retrieved and concatenated. Further, they were aligned using CLUSTALX (as described above) and their phylogeny was constructed using TreeconW software package version 1.3b with the Poisson correction model and Neighbor Joining algorithm (bootstrap value = 1000).

iii) **Tetranucleotide Correlation:** Whole-genome based tetranucleotide correlation was performed using TETRA software [70], based on which a Pearson correlation matrix was constructed. This was followed by hierarchial clustering on the resultant matrix using MeV4.9.0 [39] and finally a dendrogram was constructed in MEGA4 [71].

iv) **Average Nucleotide Identity (ANI):** This method includes all possible pairwise comparisons between these genomes as described by Konstantinidis and Tiedje (2005) [18]. Pearson correlation matrices were constructed from these ANI values, which were then used to perform hierarchical clustering followed by a dendrogram construction as described above.

Identification of genes under diversifying natural selection
Orthologs, genes involved in the degradation of aromatic compounds including HCH, and genes for transposable elements were analyzed for positive selection by extracting their sequences and performing codon by codon alignment on CLUSTALX [67]. These dN/dS and dS values, calculated for each gene pair using Hyphy 2.1.2 [72], were plotted to show the time-independent evolution of the genes.

Arrangement and diversification of the *lin* catabolic system
The Artemis Comparison Tool (Web-ACT) [73] was used to compare the arrangement of the *lin* genes and proximal genetic mobility elements such as IS*6100* with

reference to *lin* arrangement in *S. japonicum* UT26S. After constructing a database of the contigs for each strain, genes for HCH degradation were extracted using BLASTN [59], and the percent identity to the respective gene in the archetypal strain UT26S was used as a measure of genetic divergence. This divergence was plotted in addition to copy number values for each gene in each strain using the R package ggplot2 [74]. Principle component analysis (PCA) with the copy number and divergence data was then done with the R package FactoMineR [75], with HCH degradation plotted as a supplementary discrete variable (0- complete non degrader, 1- partial degrader, 2- full degrader), followed by a plot construction with ggplot2. Recruitment plots of the raw reads of the six *Sphingobium* spp. mapped against the sequence of all the plasmids of *Sphingomonas* sp MM-1 (extracted from NCBI) were created using MUMmer 3.23 [76].

Availability of supporting data
The supporting data has been deposited in Dryad (http://datadryad.org/) with doi:10.5061/dryad.g7t27.

Additional file

> **Additional file 1: Table S1.** Genes cluster identified for the degradation of aromatic hydrocarbons. **Table S2.** *lin* genes copy number within the *Sphingobium* genomes.

Author details
[1]Room No. 115, Molecular Biology Laboratory, Department of Zoology, University of Delhi, Delhi 110007, India. [2]Interdisciplinary Centre for Plant Genomics & Department of Plant Molecular Biology, University of Delhi, South Campus, New Delhi, India. [3]Argonne National Laboratory, 9700 South Cass Avenue, Argonne, IL 60439, USA. [4]Department of Ecology and Evolution, University of Chicago, 5640 South Ellis Avenue, Chicago, IL 60637, USA.

References

1. Takeuchi M, Hamana K, Hiraishi A: **Proposal of the genus *Sphingomonas* sensustricto and three new genera, *Sphingobium*, *Novosphingobium* and *Sphingopyxis*, on the basis of phylogenetic and chemotaxonomic analyses**. *Int J Syst Evol Microbiol* 2001, **51**:1405–1417.
2. Maruyama T, Park HD, Ozawa K, Tanaka Y, Sumino T, Hamana K, Hiraishi A, Kato K: ***Sphingosinicella microcystinivorans* gen. nov., sp. nov., a microcystin-degrading bacterium**. *Int J Syst Evol Microbiol* 2006, **56**:85–89.
3. Balkwill DL, Fredrickson J, Romine M: **From *Sphingomonas* and Related Genera**. In *The Prokaryotes: A Handbook on the Biology of Bacteria*. Volume 7. Edited by Stackebrandt E. Singapore: Springer; 2006:605–629.
4. Li YF: **Global technical hexachlorocyclohexane usage and its contamination consequences in the environment: from 1948 to 1997**. *Sci Total Environ* 1999, **232**:121–158.
5. Vijgen J, Yi LF, Forter M, Lal R, Weber R: **The legacy of lindane and technical HCH production**. *Organohalog Comp* 2006, **68**:899–904.
6. Lal R, Pandey G, Sharma P, Kumari K, Malhotra S, Pandey R, Raina V, Kohler HPE, Holliger C, Jackson C, Oakeshott JG: **The biochemistry of microbial degradation of hexachlorocyclohexane (HCH) and prospects for bioremediation**. *Microbiol Mol Biol Rev* 2010, **74**:58–80.
7. Boltner D, Moreno-Morillas S, Ramos JL: **16S rDNA phylogeny and distribution of *lin* genes in novel hexachlorocyclohexane-degrading *Sphingomonas* strains**. *Environ Microbiol* 2005, **7**:1329–1338.
8. Dadhwal M, Singh A, Prakash O, Gupta SK, Kumari K, Sharma P, Jit S, Verma M, Holliger C, Lal R: **Proposal of biostimulation for hexachlorocyclohexane (HCH)-decontamination and characterization of culturable bacterial community from high-dose point HCH-contaminated soils**. *J Appl Microbiol* 2009, **106**:381–392.
9. Sangwan N, Lata P, Dwivedi V, Singh A, Niharika N, Kaur J, Anand S, Malhotra J, Jindal S, Nigam A, Lal D, Dua A, Saxena A, Garg N, Verma M, Kaur J, Mukherjee U, Gilbert JA, Dowd SE, Raman R, Khurana P, Khurana JP, Lal R: **Comparative metagenomic analysis of soil microbial communities across three hexachlorocyclohexane contamination levels**. *PLoS ONE* 2012, **7**:e46219.
10. Sangwan N, Verma H, Kumar R, Negi V, Lax S, Khurana P, Khurana JP, Gilbert JA, Lal R: **Reconstructing an ancestral genotype of two hexachlorocyclohexane degrading *Sphingobium* species using metagenomic sequence data**. *ISME J* 2013, doi: 10.1038/ismej.2013.153.
11. Nagata Y, Miyauchi K, Takagi M: **Complete analysis of genes and enzymes for gamma-hexachlorocyclohexane degradation in *Sphingomonas paucimobilis* UT26**. *J Ind Microbiol Biotechnol* 1999, **23**:380–390.
12. Nagata Y, Endo R, Ito M, Ohtsubo Y, Tsuda M: **Aerobic degradation of lindane (γ-hexachlorocyclohexane) in bacteria and its biochemical and molecular basis**. *Appl Microbiol Biotechnol* 2007, **76**:741–752.
13. Sharma P, Pandey R, Kumari K, Pandey G, Jackson CJ, Russell RJ, Oakeshott JG, Lal R: **Kinetic and sequence-structure-function analysis of known LinA variants with different hexachlorocyclohexane isomers**. *PLoS ONE* 2011, **6**:e25128.
14. Geueke B, Garg N, Ghosh S, Fleischmann T, Holliger C, Lal L, Kohler HPE: **Metabolomics of hexachlorocyclohexane (HCH) transformation: ratio of LinA to LinB determines metabolic fate of HCH isomers**. *Environ Microbiol* 2013, **15**:1040–1049.
15. Aylward FO, McDonald BR, Adams SM, Valenzuela A, Schmidt RA, Goodwin LA, Woyke TA, Currie CA, Suen G, Poulsen M: **Comparison of 26 sphingomonad genomes reveals diverse environmental adaptations and biodegradative capabilities**. *Appl Environ Microbiol* 2013, **79**:3724–3733.
16. Sorek R, Lawrence CM, Wiedenheft B: **CRISPR-mediated adaptive immune system in bacteria and archaea**. *Annu Rev Biochem* 2013, **82**:237–266.
17. Bhaya D, Davison M, Barrangou R: **CRISPR-Cas systems in bacteria and archaea: versatile small RNAs for adaptive defense and regulation**. *Annu Rev Genet* 2011, **45**:273–297.
18. Konstantinidis K, Tiedje J: **Genomic insights that advance the species definition for prokaryotes**. *PNAS* 2004, **102**:2567–2572.
19. Nagata Y, Natsui S, Endo R, Ohtsubo Y, Ichikawa N, Ankai A, Oguchi A, Fukui S, Fujita N, Tsuda M: **Genomic organization and genomic structural rearrangements of *Sphingobium japonicum* UT26S, an archetypal γ-hexachlorocyclohexane-degrading bacterium**. *Enzyme Microb Technol* 2011, **49**:499–508.
20. Jit S, Dadhwal M, Kumari H, Jindal S, Kaur J, Lata P, Niharika N, Lal D, Garg N, Gupta SK, Sharma P, Bala K, Singh A, Vijgen J, Weber R, Lal R: **Evaluation of

hexachlorocyclohexane contamination from the last lindane production plant operating in India. *Environ Sci Pollut Res Int* 2011, **18**:586–597.

21. Endo R, Ohtsubo Y, Tsuda N, Nagata Y: **Identification and characterization of genes encoding a putative ABC-type transporter essential for utilization of gamma-hexachlorocyclohexane in *Sphingobium japonicum* UT26.** *J Bacteriol* 2007, **189**:3712–3720.

22. Ninfa AJ, Magasanik B: **Covalent modification of the glnG product, NRI, by the glnL product, NRII, regulates the transcription of the glnALG operon in Escherichia coli.** *Proc Natl Acad Sci U S A* 1986, **83**:5909–5913.

23. Scott N, Hess M, Bouskill NJ, Mason OU, Jansson JK, Gilbert JA: **The microbial nitrogen cycling potential is impacted by polyaromatic hydrocarbon pollution of marine sediments.** *Front Microbiol* 2014, **5**: doi:10.3389/fmicb.2014.00108.

24. Ninfa AJ, Ninfa EG, Lupas AN, Srock A, Magasanik B, Stock J: **Crosstalk between bacterial chemotaxis signal transduction proteins and regulators of transcription of the Ntr regulon: evidence that nitrogen assimilation and chemotaxis are controlled by a common phosphotransfer mechanism.** *Proc Natl Acad Sci U S A* 1988, **85**:5492–5496.

25. Pal R, Bala S, Dhingra G, Prakash O, Dadhwal M, Kumar M, Prabagaran SR, Shivaji S, Cullum J, Holliger C, Lal R: **The hexachlorocyclohexane-degrading bacterial strains *Sphingomonas paucimobilis* B90A, UT26S and Sp+ having similar *lin* genes are three distinct species, *Sphingobium indicum* sp. nov; *S. japonicum* sp. nov; and *S. francense* sp. nov. and reclassification of [*Sphingomonas*] *chungbukensis* as *Sphingobium chungbukense* comb. nov.** *Int J Syst Evol Microbiol* 2005, **55**:1965–1972.

26. Kumari H, Gupta SK, Jindal S, Katoch P, Lal R: **Description of *Sphingobium lactosutens* sp. nov., isolated from a hexachlorocyclohexane dump site and *Sphingobium abikonense* sp. nov. isolated from oil contaminated soil.** *Int J Syst Evol Microbiol* 2009, **59**:2291–2296.

27. Dadhwal M, Jit S, Kumari H, Lal R: ***Sphingobium chinhatense* sp. nov., a hexachlorocyclohexane (HCH) degrading bacterium isolated from an HCH dump site.** *Int J Syst Evol Microbiol* 2009, **59**:3140–3144.

28. Singh A, Lal R: **A novel hexachlorocyclohexane degrading bacterium Sphingobium ummariense sp. nov. isolated from HCH contaminated soil.** *Int J Syst Evol Microbiol* 2009, **59**:162–166.

29. Bala K, Sharma P, Lal R: ***Sphingobium quisquiliarum* sp. nov., P25ᵀ a hexachlorocyclohexane (HCH) degrading bacterium isolated from HCH contaminated soil.** *Int J Syst Evol Microbiol* 2010, **60**:429–433.

30. Kaur J, Moskalikova H, Niharika N, Sedlackova M, Hampl A, Damborsky J, Prokop Z, Lal R: ***Sphingobium baderi* sp. nov., isolated from a hexachlorocyclohexane (HCH) dumpsite in Spolana.** *Int J Syst Evol Microbiol* 2012, **63**:673–678.

31. Dogra C, Raina V, Pal R, Suar M, Lal S, Gartemann KH, Holliger C, van der Meer JR, Lal R: **Organization of *lin* genes and IS*6100* among different strains of hexachlorocyclohexane-degrading *Sphingomonas paucimobilis*: evidence for horizontal gene transfer.** *J Bacteriol* 2004, **186**:2225–2235.

32. Mohn WW, Mertens B, Neufeld J, De Lorenzo V: **Distribution and phylogeny of hexachlorocyclohexane-degrading bacteria in soils from Spain.** *Environ Microbiol* 2006, **8**:60–68.

33. Malhotra S, Sharma P, Kumari H, Singh A, Lal R: **Localization of HCH catabolic genes (*lin* genes) in *Sphingobium indicum* B90A.** *Indian J Microbiol* 2007, **47**:271–275.

34. Gai Z, Wang X, Tang H, Tai C, Tao F, Wu G, Xu P: **Genome sequence of *Sphingobium yanoikuyae* XLDN2-5, an efficient carbazole-degrading strain.** *J Bacteriol* 2011, **193**:6404–6405.

35. Tabata M, Ohtsubo Y, Ohhata S, Tsuda M, Nagata Y: **Complete genome sequence of the gamma-hexachlorohexane-degrading bacterium *Sphingomonas* sp. Strain MM-1.** *Genome Announc* 2013, **1**:e00247-13.

36. Kumari R, Subudhi S, Suar M, Dhingra G, Raina V, Dogra C, Lal S, Holliger C, van der Meer JR, Lal R: **Cloning and characterization of *lin* genes responsible for the degradation of hexachlorocyclohexane isomers in *Sphingomonas paucimobilis* strain B90.** *Appl Environ Microbiol* 2002, **68**:6021–6028.

37. Suar M, van der Meer JR, Lawlor K, Holliger C, Lal R: **Dynamics of multiple *lin* gene expression in *Sphingomonas paucimobilis* B90A in response to different hexachlorocyclohexane isomers.** *Appl Environ Microbiol* 2004, **70**:6650–6656.

38. Nagata Y, Mori K, Takagi M, Murzin AG, Damborsky J: **Identification of protein fold and catalytic residues of γ-hexachlorocyclohexane dehydrochlorinase LinA.** *Proteins* 2001, **45**:471–477.

39. Sharma P, Jindal S, Bala K, Kumari K, Niharika N, Kaur J, Pandey G, Pandey R, Russell RJ, Oakeshott JG, Lal R: **Functional screening of enzymes and**

40. Nagata Y, Hatta T, Imai R, Kimbara K, Fukuda M, Yano K, Takagi M: **Purification and characterization of γ-hexachlorocyclohexane (γ-HCH) dehydrochlorinase (LinA) from *Pseudomonas paucimobilis*.** *Biosci Biotechnol Biochem* 1993, **59**:1582–1583.

41. Ceremonie H, Boubakri H, Mavingui P, Simonet P, Vogel TM: **Plasmid-encoded γ-hexachlorocyclohexane degradation genes and insertion sequences in *Sphingobium francense* (ex-*Sphingomonas paucimobilis* Sp+).** *FEMS Microbiol Lett* 2006, **257**:243–252.

42. Wu J, Hong Q, Han P, He J, Li S: **A gene *lin*B2 responsible for the conversion of β-HCH and 2,3,4,5,6-pentachlorocyclohexanol in *Sphingomonas* sp. BHC-A.** *Appl Microbiol Biotechnol* 2007, **73**:1097–1105.

43. Ito M, Prokop Z, Klvana M, Otsubo Y, Tsuda M, Damborsky J, Nagata Y: **Degradation of beta-hexachlorocyclohexane by haloalkane dehalogenase LinB from gamma-hexachlorocyclohexane-utilizing bacterium *Sphingobium* sp. MI1205.** *Arch Microbiol* 2007, **188**:313–325.

44. Glavinas H, Krajcsi P, Cserepes J, Sarkadi B: **The role of ABC transporters in drug resistance, metabolism and toxicity.** *Curr Drug Deliv* 2004, **1**:27–42.

45. Anand S, Sangwan N, Lata P, Kaur J, Dua A, Singh AK, Verma M, Kaur J, Khurana JP, Khurana P, Mathur S, Lal R: **Genome sequence of *Sphingobium indicum* B90A, a hexachlorocyclohexane-degrading bacterium.** *J Bacteriol* 2012, **194**:4471–4472.

46. Nagata Y, Ohtsubo Y, Endo R, Ichikawa N, Ankai A, Oguchi A, Fukui S, Fujita N, Tsuda M: **Complete genome sequence of the representative γ-hexachlorocyclohexane-degrading bacterium *Sphingobium japonicum* UT26S.** *J Bacteriol* 2010, **192**:5852–5853.

47. Masai E, Kamimura N, Kasai D, Oguchi A, Ankai A, Fuki S, Fukui S, Takahashi M, Yashiro I, Sasaki H, Harada T, Nakamura S, Katano Y, Narita-Yamada S, Nakazawa H, Hara H, Katayama Y, Fukuda M, Yamazaki S, Fujitab N: **Complete genome sequence of *Sphingobium* sp. strain SYK-6, a degrader of lignin-derived biaryls and monoaryls.** *J Bacteriol* 2012, **194**:534–535.

48. Sambrook J, Fritsch EJ, Maniatis T, Maniatis T (Eds): *Molecular Cloning: A Laboratory Manual. Volume 2.* 2nd edition. New York: Cold Spring Harbor Laboratory Press; 1989.

49. Simpson JT, Wong K, Jackman SD, Schein JE, Jones SJ, Birol I: **ABySS: a parallel assembler for short read sequence data.** *Genome Res* 2009, **19**:1117–1123.

50. Li H, Durbin R: **Fast and accurate short read alignment with Burrows-Wheeler Transform.** *Bioinformatics* 2009, **25**:1754–1760.

51. Kaur J, Verma H, Tripathi C, Khurana JP, Lal R: **Draft genome sequence of a hexachlorocyclohexane-degrading bacterium, *Sphingobium baderi* strain LL03ᵀ.** *Genome Announc* 2013, **1**:e00751-13.

52. Kumar R, Dwivedi V, Negi V, Khurana JP, Lal R: **Draft genome sequence of *Sphingobium lactosutens* strain DS20 isolated from an hexachlorocyclohexane (HCH) dumpsite.** *Genome Announc* 2013, **1**:00753-13.

53. Niharika N, Sangwan N, Ahmad S, Singh P, Khurana JP, Lal R: **Draft genome sequence of *Sphingobium chinhatense* strain IP26ᵀ isolated from the hexachlorocyclohexane dumpsite.** *Genome Announc* 2013, **1**:00680-13.

54. Singh AK, Sangwan N, Sharma A, Gupta V, Khurana JP, Lal R: **Draft genome sequence of *Sphingobium quisquiliarum* P25ᵀ, a novel hexachlorocyclohexane (HCH)- degrading bacterium isolated from the HCH dumpsite.** *Genome Announc* 2013, **1**:00717-13.

55. Kohi P, Dua A, Sangwan N, Oldach P, Khurana JP, Lal R: **Draft genome sequence of *Sphingobium ummariense* strain RL-3, a hexachlorocyclohexane-degrading bacterium.** *Genome Announc* 2013, **1**:00956-13.

56. Mukherjee U, Kumar R, Mahato NK, Khurana JP, Lal R: **Draft genome sequence of *Sphingobium* sp. HDIPO4, an avid degrader of hexachlorocyclohexane.** *Genome Announc* 2013, **1**:00749-13.

57. Delcher AL, Bratke KA, Powers EC, Salzberg SL: **Identifying bacterial genes and endosymbiont DNA with Glimmer.** *Bioinformatics* 2007, **23**:673–679.

58. Aziz RK, Bartels D, Best AA, DeJongh M, Disz T, Edwards RA, Formsma K, Gerdes S, Glass EM, Kubal M, Meyer F, Olsen GJ, Olson R, Osterman AL, Overbeek RA, McNeil LK, Paarmann D, Paczian T, Parrello B, Pusch GD, Reich C, Stevens R, Vassieva O, Vonstein V, Wilke A, Zagnitko O: **The RAST server: rapid annotations using subsystems technology.** *BMC Genomics* 2008, **9**:75.

59. Altschul SF, Gish W, Miller W, Myers EW, Lipman DJ: **Basic local alignment search tool.** *J Mol Biol* 1990, **215**:403–410.

60. Li W, Godzik A: **Cd-hit: a fast program for clustering and comparing large sets of protein or nucleotide sequences.** *Bioinformatics* 2006, **22**:1658–1659.

61. Vallenet D, Belda E, Calteau A, Cruveiller S, Engelen S, Lajus A, Fèvre FL, Longin C, Mornico D, Roche D, Rouy Z, Salvignol G, Scarpelli C, Smith AAT, Weiman M, Médigue C: **MicroScope—an integrated microbial resource for the curation and comparative analysis of genomic and metabolic data.** *Nucleic Acids Res* 2013, **41**:D636–D647.

62. Moriya Y, Itoh M, Okuda S, Yoshizawa A, Kanehisa M: **KAAS: an automatic genome annotation and pathway reconstruction server.** *Nucleic Acids Res* 2007, **35**:W182–W185.

63. Ye Y, Doak TG: **A parsimony approach to biological pathway reconstruction/inference for genomes and metagenomes.** *PLoS Comput Biol* 2009, **5**:e1000465.

64. Saeed AI, Sharov V, White J, Li J, Liang W, Bhagabati N, Braisted J, Klapa M, Currier T, Thiagarajan M, Sturn A, Snuffin M, Rezantsev A, Popov D, Ryltsov A, Kostukovich E, Borisovsky I, Liu Z, Vinsavich A, Trush V, Quackenbush J: **TM4: a free, open-source system for microarray data management and analysis.** *Biotechniques* 2003, **34**:374–378.

65. Langille MGI, Brinkman FSL: **IslandViewer: an integrated interface for computational identification and visualization of genomic islands.** *Bioinformatics* 2009, **25**:664–665.

66. Grissa I, Vergnaud G, Pourcel C: **CRISPRFinder: a web tool to identify clustered regularly interspaced short palindromic repeats.** *Nucleic Acids Res* 2007, **35**:W52–W57.

67. Larkin MA, Blackshields G, Brown NP, Chenna R, McGettigan PA, McWilliam H, Valentin F, Wallace IM, Wilm A, Lopez R, Thompson JD, Gibson TJ, Higgins DG: **Clustal W and Clustal X version 2.0.** *Bioinformatics* 2007, **23**:2947–2948.

68. Van de Peer Y, De Wachter Y: **TREECON for Windows: a software package for the construction and drawing of evolutionary trees for the Microsoft Windows environment.** *Comput Applic Biosci* 1994, **10**:569–570.

69. Jukes TH, Cantor CR: **Evolution of protein molecules," in Munro (ed.).** *Mammalian Protein Metabolism* 1969, **3**:21–132.

70. Teeling H, Waldmann J, Lombardot T, Bauer M, Glöckner FO: **TETRA: a web-service and a stand-alone program for the analysis and comparison of tetranucleotide usage patterns in DNA sequences.** *BMC Bioinformatics* 2004, **5**:163.

71. Tamura K, Dudley J, Nei M, Kumar S: **MEGA4: Molecular Evolutionary Genetics Analysis (MEGA) software version 4.0.** *Mol Bioland Evol* 2007, **24**:1596–1599.

72. Pond SLK, Frost SDW, Muse SV: **HyPhy: hypothesis testing using phylogenies.** *Bioinformatics* 2005, **21**:676–679.

73. Carver TJ, Rutherford KM, Berriman M, Rajandream MA, Barrell BG, Parkhill J: **ACT: the artemis comparison tool.** *Bioinformatics* 2005, **16**:3422–3433.

74. Wickham H: *Ggplot2: Elegant Graphics for Data Analysis.* New York: Springer; 2009:213.

75. Le S, Josse J, Husson F: **FactoMineR: an R package for multivariate analysis.** *J Stat Softw* 2008, **25**:1–18.

76. Kurtz S, Phillippy A, Delcher AL, Smoot M, Shumway M, Antonescu C, Salzberg SL: **Versatile and open software for comparing large genomes.** *Genome Biol* 2004, **5**:12.